International Journal of General Medicine

Dovepress
Taylor & Francis Group

Open Access Full Text Article

ORIGINAL RESEARCH

Study of Macular Microvascular Changes in Patients with Symptomatic Lacunar Cerebral Infarction Using Viaoptical Coherence Tomography Angiography (OCTA)

Meishuang Li[1–4,*], Huiyu Xi[1,3,4,*], Rongrong Guan[5,*], Yalu Liu[1,3,4], Lina Guan[1,3,4], Dandan Zong[1,4,6], Nuan Wang[1,4], Haiyang Liu[1,3,4]

[1]Department of Ophthalmology, Affiliated Xuzhou Municipal Hospital of Xuzhou Medical University, Xuzhou, People's Republic of China; [2]Department of Ophthalmology, Lianyungang Eye Hospital, Lianyungang, People's Republic of China; [3]Department of Ophthalmology, Eye Disease Prevention and Treatment Institute, Xuzhou, People's Republic of China; [4]Department of Ophthalmology, Xuzhou First People's Hospital, Xuzhou, People's Republic of China; [5]Department of Ophthalmology, Affiliated Suqian Hospital of Xuzhou Medical University, Suqian, People's Republic of China; [6]Department of Ophthalmology, Xuzhou Jiawang District People's Hospital, Xuzhou, People's Republic of China

*These authors contributed equally to this work

Correspondence: Haiyang Liu, Affiliated Xuzhou Municipal Hospital of Xuzhou Medical University, Xuzhou First People's Hospital, Eye Disease Prevention and Treatment Institute of Xuzhou, No. 269 Daxue Road, Tongshan District, Xuzhou, 221116, People's Republic of China, Tel +8613685167216, Email liuhaiyang86@126.com; Nuan Wang, Affiliated Xuzhou Municipal Hospital of Xuzhou Medical University, Xuzhou First People's Hospital, No. 269 Daxue Road, Tongshan District, Xuzhou, 221116, People's Republic of China, Email 1279814072@qq.com

Objective: To investigate retinal and choroidal vascular density (VD) changes in the macular region of patients with symptomatic lacunar cerebral infarction (LI) and assess whether these changes can predict symptomatic LI.

Methods: This cross-sectional study included 49 symptomatic LI patients (49 eyes) and 51 healthy controls (51 eyes). OCTA was employed to measure retinal VD in the superficial capillary plexus (SCP) and deep capillary plexus (DCP), as well as the ganglion cell complex (GCC) thickness. Enhanced depth imaging optical coherence tomography (EDI-OCT) was utilized to calculate the choroidal vascular index (CVI).

Results: Significant differences were observed in macular VD of the SCP and DCP, GCC thickness, and CVI, systolic pressure, diastolic pressure, between the symptomatic LI and control groups ($p < 0.05$). Binary logistic regression analysis indicated that lower VD in the SCP and DCP, along with reduced GCC thickness, elevated diastolic blood pressure, were significantly associated with symptomatic LI (OR < 1, $p < 0.05$). Receiver operating characteristic (ROC) curve analysis showed that the area under the curve (AUC) was higher for SCP total vessel density and GCC thickness, while the whole VD of SCP+GCC thickness had the highest area under the curve (AUC =0.880, sensitivity =87.80% and specificity =74.50%).

Conclusion: In patients with symptomatic LI, reductions in VD within the SCP and DCP, along with decreased GCC thickness and CVI, were observed. These diminished vascular densities in the SCP and reduced GCC thickness may serve as predictive markers for symptomatic LI.

Keywords: symptomatic lacunar cerebral infarction, vascular density, thickness of ganglion cell complex, optical coherence tomography vascular imaging technology

Introduction

Lacunar cerebral infarction is defined as a clinical syndrome characterised by the occurrence of small perforating arteries in the cerebral hemisphere or deep brainstem undergoing pathological changes in the vascular wall. These changes are precipitated by long-term hypertension and other risk factors, ultimately leading to occlusion of the lumen and ischaemic necrosis of the cerebral tissue supplying the artery, resulting in neurological deficits.[1] Stroke is recognized as the third

Received: 9 May 2025
Accepted: 26 August 2025
Published: 9 September 2025

Graphical Abstract

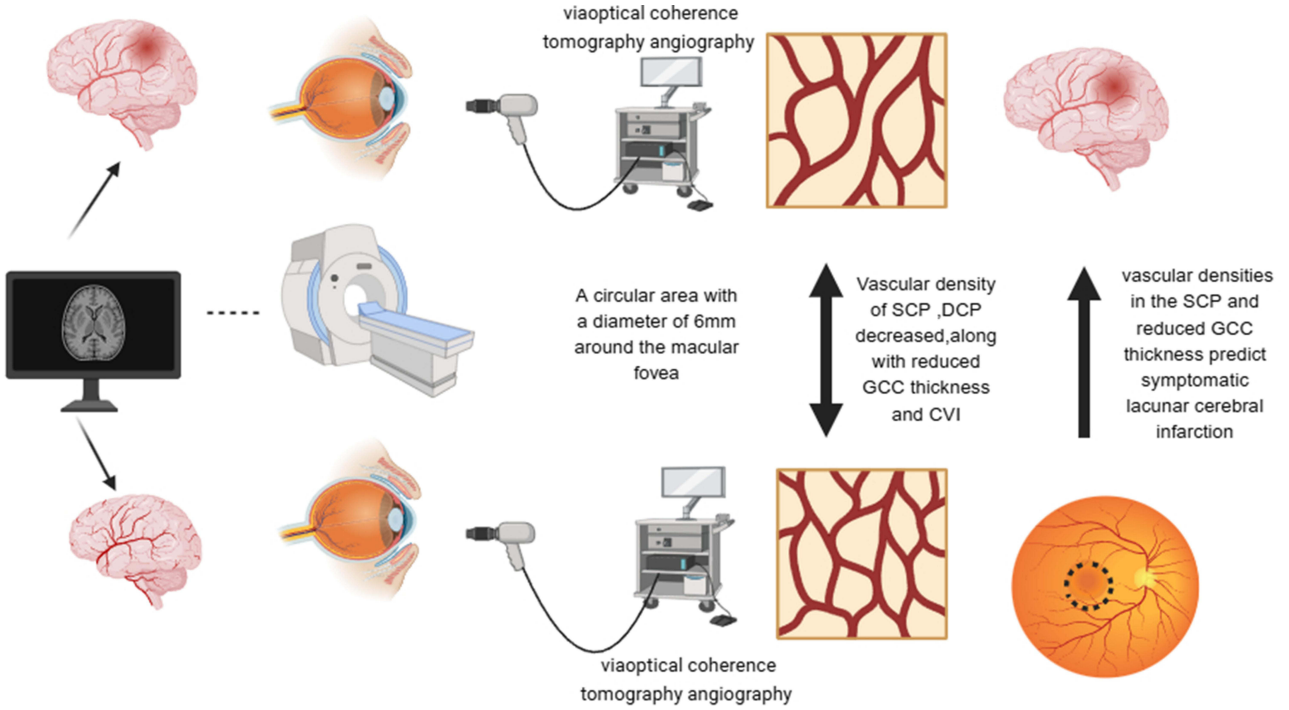

primary cause of disability worldwide and the second major cause of death. The high recurrence rate of ischaemic stroke has become a serious global problem, with lacunar infarction accounting for over 25% of all cases of ischaemic stroke in the Chinese population.[2] Currently, the diagnosis and grading of cerebrovascular diseases rely on multiple indicators, such as blood test results, and radiographic imaging, such as magnetic resonance imaging (MRI) and positron emission tomography (PET),[3] which are expensive to perform and pose radiation risks. However, owing to the transparency of the refractive medium in the eye, the retina has become the only ocular nerve tissue in the human body that can be directly observed under noninvasive conditions and has therefore received widespread attention from researchers in the field of medical biology.[4,5] Retinal blood vessels exhibit characteristics that are analogous to those of cerebral microvessels, both embryologically, anatomically and physiologically, and thus represent a valuable model with which to study alterations in brain microvessels.[6] Early research revealed that pathological changes, including retinal haemorrhage, microangiomas and changes in retinal diameter, could be observed in the retinas of patients with early-stage cerebrovascular disease.[7–9] There is a substantial body of evidence indicating that microvascular impairment, indicative of small vessel disease, is the primary cause of ischaemic stroke.[10] Due to the limited depth of fundus photography, retinal capillary imaging is constrained. OCTA, a non-invasive examination modality, has been shown to detect moving blood cells in blood vessels, obtain layered images of retinal blood flow density, display data parameters, and quantitatively analyse microvessels at different levels.[11,12] A significant body of research has been conducted using OCTA technology to detect, screen, and predict other systemic diseases, including cardiovascular disease, Parkinson's disease, and cerebral small vessel disease, through the analysis of retinal microvessels.[13–15]

In 2011, a study found that the more sparse the retinal vessels, the more severe the brain tissue hypoxia, and the higher the stroke incidence, which can predict the mortality rate of stroke in the elderly.[16] In 2021 a study indicated that in high-risk individuals before the onset of cerebrovascular disease, the presence of relatively sparse retinal vessels can lead to early intervention, reducing the incidence and severity of stroke.[17] In 2021, an OCTA study on retinal blood flow in patients with carotid artery stenosis revealed that the retinal microvascular system may reflect changes in cerebral hemodynamics in these patients, suggesting that OCTA can serve as a potential non-invasive quantitative screening tool

for assessing cerebral hemodynamic impairment.[18] In 2024, it was found that patients with recurrent cerebrovascular events had wider retinal vein diameters and smaller artery diameters, indicating the potential value of retinal vessel diameter (especially retinal vein diameter) as a predictor of recurrent cerebrovascular events in patients with acute ischemic stroke.[19] Therefore, retinal microvessels can serve as a potential biomarker for predicting cerebrovascular diseases.

In this study, OCTA and EDI-OCT combined technology were used to observe the changes of retinal microvessels and choroidal vessels in the macular region of symptomatic LI patients, which provided a non-invasive and convenient evaluation method for early diagnosis of LI, which was beneficial to the prevention and treatment of LI.

Materials and Methods

Study Participants

This cross-sectional study comprised 49 patients (49 eyes) with symptomatic lacunar cerebral infarction, as diagnosed by neurological examination, between January 2023 and May 2023 at the Affiliated Xuzhou Municipal Hospital of Xuzhou Medical University (Xuzhou First People's Hospital). Fifty- One healthy individual (51 eyes) who underwent a physical examination at the Physical Examination Center of the Xuzhou First People's Hospital during the same period and were excluded from lacunar cerebral infarction through magnetic resonance imaging (MRI) were selected to form the control group. Members of the control group showed no prior history or indications of stroke. Approval for the study was granted by the Ethics Committee of the Affiliated Xuzhou Municipal Hospital of Xuzhou Medical University (Xuzhou First People's Hospital) (Ethics Number: xyy11 (2023) 057), and all participants provided their informed written consent.

The inclusion criteria were as follows: (1) Subjects with lacunar cerebral infarction (lacunar cerebral infarction confirmed by cranial CT combined with MRI) aged 50–80 years old who are being treated in our hospital meet the diagnostic criteria for lacunar stroke;[1] (2) Subjects must not have any central nervous defects, such as Alzheimer's disease, congenital cerebrovascular disease, history of epilepsy, or any other clear causes of stroke, including vasculitis, smoky disease, etc. Subjects must also not have any cerebral haemorrhage, hydrocephalus, or brain tumours; (3) Subjects must be able to cooperate with OCTA examination; (4) Subjects who understood the purpose of the study, were willing participants, had good compliance and signed a consent form.

The exclusion criteria were as follows: (1) Subjects with refractive media opacity who were unable to undergo fundus photography and OCTA examination; (2) Subjects with additional eye diseases beyond mild cataracts, including macular degeneration, any history of retinal surgery or laser photocoagulation treatment, and high myopia with a refractive error exceeding ± 6.0 D; (3) Subjects with other systemic vascular diseases unrelated to cerebral infarction, such as diabetes or systemic lupus erythematosus; (4) Subjects who were unable to cooperate with any of the examinations.

Data Collection

Patient data included basic demographic information (age, gender,) and medical history (ocular diseases, diabetes, hypertension, cholesterol).

General Ocular Assessment and Evaluation of Indices Related to Fundus Microvascular Alterations

All participants underwent comprehensive ophthalmic examinations, including binocular assessment. However, the analysis utilized data exclusively from the left eye. The examination protocol included refractive measurement, intraocular pressure (IOP), unaided visual acuity, axial length, and best-corrected visual acuity (BCVA), along with slit-lamp examination, funduscopy, and non-dilated color fundus photography focusing on the posterior pole of each eye. These evaluations ensured only eligible participants were included in the study. In addition, OCTA and EDI-OCT tests were performed.

The OCTA system (AngioVue, RTVue XR Avanti, Optovue, Fremont, CA, USA software version 2018.0.0.18) utilizes frequency-domain OCTA technology combined with spectral amplitude de-correlation angiography (SSADA) algorithm to achieve retinal vascular imaging. The system emits near-infrared laser with a central wavelength of 840 nm and 45 nm

bandwidth to penetrate retinal tissue, performing axial scanning at a high speed of 70,000 A-scan/second (70 kHz) to rapidly acquire retinal layering signals. Within a 6×6 mm scanning area, the system performs two consecutive volumetric scans, each containing 400 B-scan slices (each B-slice composed of 400 A-slices), repeating B-slice pairs at the same position to reduce motion artifacts. The SSADA algorithm intelligently distinguishes static tissues (low de-correlation) from blood flow signals (high de-correlation) by analyzing adjacent B-slices' amplitude de-correlation. Its spectral processing technology decomposes OCT signals into multiple sub-frequency bands, significantly suppressing noise and enhancing the signal-to-noise ratio of blood flow signals. The built-in automatic stratification algorithm accurately identifies and segments interretinal reflection differences, automatically exporting vascular density and retinal thickness data for macula and perimacular capillary plexus. Recorded parameters include perimeter and area of the foveal avascular zone (FAZ), as well as vascular density values for superficial capillary plexus (SCP) and deep capillary plexus (DCP).[20,21] The SCP is defined as the layer located 3 μm beneath the internal limiting membrane (ILM) and extends to 15 μm below the inner plexiform layer (IPL); DCP is identified as the layer situated 15–70 μm below the IPL. Use the non-flow function tool to click on the center of the avascular fovea (FAZ) for automatic measurement.[22] The measurement range is selected between 3 μm and 70 μm below the inner retinal membrane, measured in millimeters.[23] The system automatically calculates the area and perimeter parameters of the FAZ, with AI defined as the ratio of PERIM to the area of a standard circle (see Figure 1).[24,25] The ganglion cell complex (GCC) was obtained by scanning a 1 mm center of the macular fovea and covering a 6×6 mm area of the macular region. The mean thickness measurements included values from the inner limiting membrane (ILM) to the outer

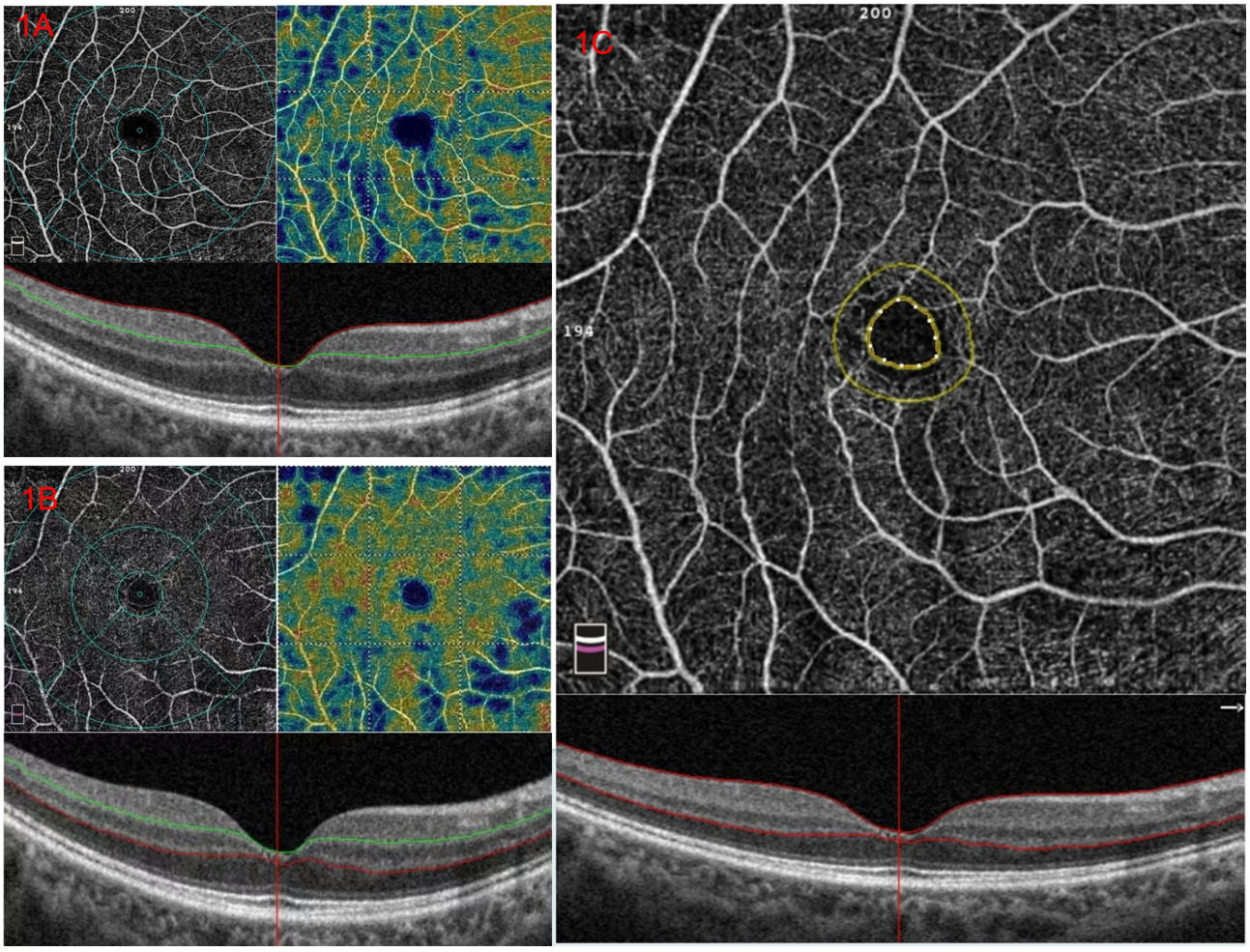

Figure 1 Structural zoning and scanning hierarchy of the macula (6 ✖ 6 mm).
Notes: The 6✖6mm structural zoning and scanning hierarchy of the macula in representative LI patients are shown, with lower density of blue blood vessels than orange blood vessels. (**A**) Superficial capillary plexus; (**B**) Deep capillary plexus; (**C**) FAZ Measurements.

boundary of the inner plexiform layer (IPL).[26] After data acquisition, the scanned images were automatically segmented by the machine into the foveal, parafoveal, and perifoveal regions, and further divided into the superficial capillary plexus (SCP) and deep capillary plexus (DCP). The foveal, parafoveal, and perifoveal regions were defined as circular areas with diameters of 1 mm, 3 mm, and 6 mm, respectively. The parafoveal and perifoveal regions were further subdivided into four quadrants using four radial divisions: the temporal, superior, nasal, and inferior regions (Figure 2A). All measurements, including SCP, DCP, GCC, and FAZ parameters, were automatically calculated by the built-in software algorithms. (2) Choroidal vascular index: All subjects underwent EDI-OCT scanning via spectral HRA-OCT (Heidelberg Engineering, Heidelberg). We have taken into account the effect of circadian rhythms on the choroid and all subjects had EDI-OCT examinations between 15:00 and 17:00. The macular fovea was designated as the centre, and the volume was scanned at 30×5, with an average of 100 frames per scan. Using the public domain software Fiji (http://fiji.sc/Fiji), the EDI-OCT images were opened in ImageJ, the correct scale was set, the greyscale image (Figure 3A) was first converted to 8 bits, the image was binarised using Niblack's automatic local thresholding (Figure 3B), The region of interest was then selected using the polygon tool over the entire length of the OCT scan (Figure 3C), and the upper boundary of the region of interest was traced along the choroid-retinal pigment epithelium junction and the lower boundary along the choroid-sclera junction to determine the total choroidal area (TCA). Finally, the images were converted back to red, green and blue images and dark pixels representing the luminal area (LA) were selected using the colour thresholding tool (Figure 3D). Total TCA and LA were measured and then CVI, defined as LA divided by TCA%, was calculated. Three separate calculations were performed and averaged for statistical analysis (see Figure 3).[27]

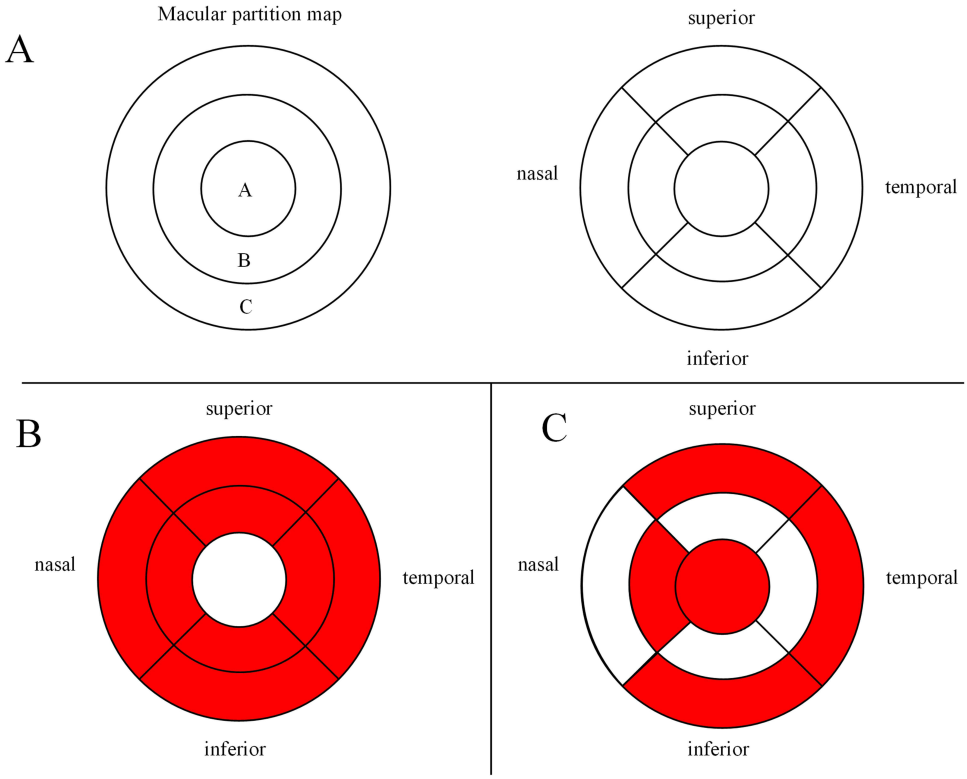

Figure 2 Schematic diagram illustrating changes in macular vascular density.
Notes: (**A**) The area within the first small ring is known as the macular fovea (**A**), the region between the first and second rings denotes the parafoveal area (**B**), and the area between the second and third rings indicates the perifoveal area (**C**). The B and C regions are further subdivided into nasal, superior, temporal, and inferior regions. (**B**) Comparison of vessel density of the SCP in the macular area between the symptomatic LI group and the control group. The red areas indicate significantly lower vessel density in the symptomatic LI group when comparison is made with the control group. Specifically, the symptomatic LI group showed a significant decrease in vessel density in the both the parafoveal and perifoveal macular areas (superior, nasal, inferior and temporal regions) compared to the control group. (**C**) Comparison of vascular density of the DCP in the macular area between the symptomatic LI group and the control group. In a comparison with the control group, the symptomatic LI group displayed a significant reduction in vascular density in Foveal area and the nasal region of the macular parafoveal area, as well as in the superior, temporal, and inferior regions of the macular perifoveal area.
Abbreviations: SCP, superficial capillary plexus; DCP, deep capillary plexus; LI, lacunar cerebral infarction.

https://doi.org/10.2147/IJGM.S534255

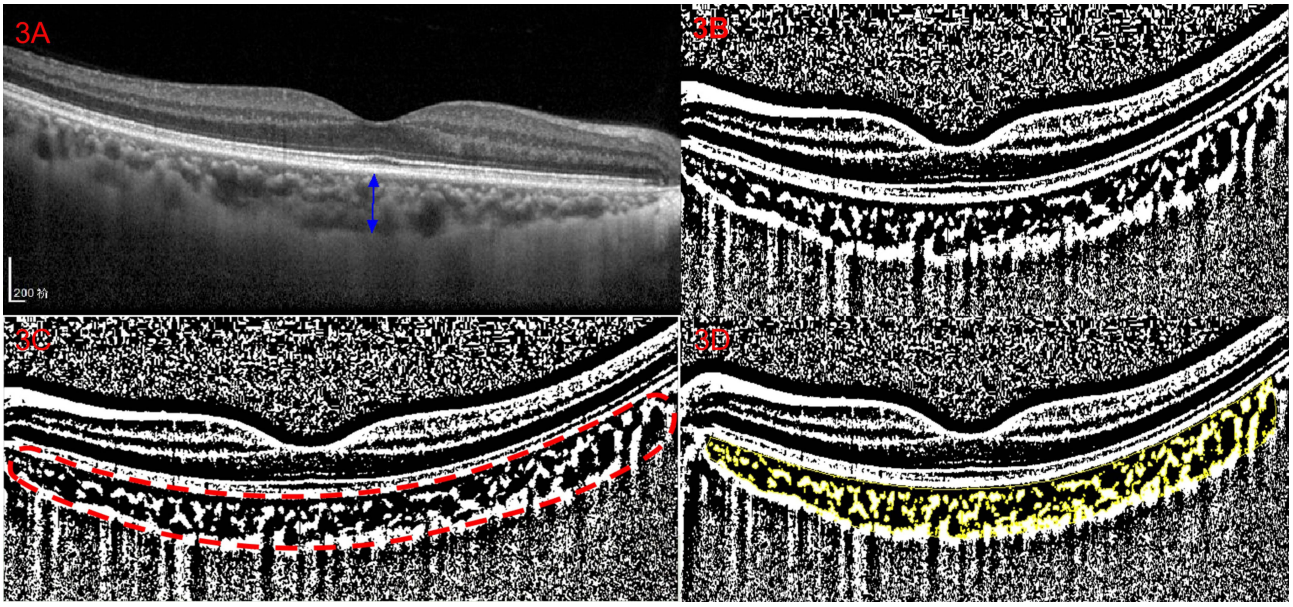

Figure 3 EDI-OCT scan the choroid and calculate CVI.
Notes: (**A**) Original EDI-OCT image of the acquisition; (**B**) binarization for image A using Niblack's automatic local thresholding; (**C**) tracing the choroidal border to determine the total area of the choroid (within the red line); (**D**) using the color thresholding tool to select dark pixels representing the lumen area.

All sans are performed on the same device to prevent inter-machine variations. OCTA and EDI-OCT examinations were performed using the same equipment by the same technician (MS.L) to ensure high consistency in testing conditions and stable results. Images with insufficient quality (scanning quality <7/10) or affected by artifacts were excluded, and all findings were validated by two ophthalmologists (YL.L & LN.G).[26] The device generates independent high-definition blood flow images for each layer, which greatly improves the efficiency of clinical examinations, and effectively corrects artifacts caused by eye movements through repeated scans and decorrelation calculations.

Statistical Methods Calculation of CVI Using Binarisation of OCT Images

SPSS version 27.0 was used for statistical analysis of the data, and the chi-squared test was used for categorical data, with results expressed as the number (percentage) of test cases. Continuous data, which followed a normal distribution, are presented as mean ± standard deviation and were analysed using the *t*-test. For data not conforming to a normal distribution, the Mann–Whitney *U*-test was used, and the results are presented as the median [quartiles]. Binary stepwise logistic regression analysis (stepwise method "Forward:LR" was selected) was applied to examine the correlation between macular microvascular changes and symptomatic LI. The receiver operating characteristic (ROC) curve of the subjects was drawn, and the area under the ROC curve (AUC) was calculated to evaluate the predictive symptomatic LI value of the parameters. P <0.05 was considered to indicate clinical significance.

Results

General Information on the Two Groups of Subjects

This study included a total of 49 subjects with symptomatic LI and 51 healthy controls. There were no statistically significant differences in age, sex, intraocular pressure, best-corrected visual acuity (BCVA), axial length, cholesterol levels, or fasting blood glucose between the two groups ($p > 0.05$). However, a statistically significant was observed in systolic and diastolic blood pressure measurements ($p < 0.05$), see Table 1.

Table 1 Comparison of General Data Between the Two Groups

	LI Group (N=49)	Control Group (N=51)	χ2/t/z	P Value
Sex (Male/female)	23(46.94%)/26(53.06%)	23(45.10%)/28(54.90%)	0.034	0.854
Age	64.00 [59.00;68.00]	63.00 [58.00;65.50]	−1.271	0.204
BCVA (LogMAR)	0.10 [0.00;0.10]	0.00 [0.00;0.10]	−1.687	0.092
Axial length	23.74±0.74	23.63±0.79	0.731	0.467
Intraocular pressure	13.90±2.33	14.66±2.15	−1.694	0.094
Systolic pressure	140.00[130.00;149.00]	136.00[128.00;141.00]	−2.012	0.044
Diastolic pressure	84.00 [79.00;90.00]	82.00 [76.50;85.50]	−2.135	0.033
Fasting blood glucose	5.28±0.41	5.32±0.39	−0.545	0.587
Cholesterol	4.44±0.82	4.15±0.64	1.950	0.054

Abbreviation: BCVA, best-corrected visual acuity.

Comparison of Macular Vascular Density and Other Parameters Amongst the Two Subject Groups

Compared with the control group, the retinal vascular density (VD) in symptomatic LI group was significantly reduced in SCP in whole, parafoveal and perifoveal area ($p < 0.05$), In the deep capillary plexus (DCP), VD was also reduced in the whole image, foveal, parafoveal, and perifoveal areas (see Table 2). In the SCP, the temporal, superior, nasal, and inferior regions of both the parafoveal and perifoveal areas showed significantly lower VD compared to the control group ($p < 0.001$) (see Table 3 and Figure 2B). In the DCP, the nasal region of the parafoveal area was significantly lower ($P = 0.027$), and the temporal, superior, and inferior regions of the perifoveal area also showed reduced VD ($P < 0.05$) (see Table 4 and Figure 2C). Additionally, GCC thickness and CVI were significantly reduced in the symptomatic LI group ($p < 0.05$). In contrast, FAZ area, PERIM, and AI showed no significant differences ($p > 0.05$) (see Table 5).

Correlation Between Macular Microvascular Parameters and the Occurrence of Symptomatic Lacunar Cerebral Infarction

The presence or absence of lacunar cerebral infarction was designated as the dependent variable, with a value of 1 assigned to the group with cerebral infarction and 0 to the group without. Statistically significant parameters, including systolic pressure, diastolic pressure, VD of both SCP and DCP, GCC thickness, and CVI, were included as independent variables. The data underwent binary stepwise logistic regression analysis, utilizing a "Forward: LR" stepwise method. The results indicated that lower VD in SCP and reduced GCC thickness in the macular areas, were significantly associated with an increase in the

Table 2 Comparison Vascular Density of SCP, DCP in the Macular Area Between the Two Subject Groups

	Vascular Density (%)	LI Group (N=49)	Control Group (N=51)	t/z	P-Value
SCP	Whole	47.10[45.20;49.70]	51.30[49.95;52.65]	−6.131	<0.001
	Foveal area	16.24±6.77	18.20±5.78	−1.563	0.121
	Parafoveal area	49.90[46.30;52.40]	53.00[51.40;54.95]	−5.045	<0.001
	Perifoveal area	47.90[45.90;50.00]	52.00[50.35;53.25]	−5.982	<0.001
DCP	Whole	48.17±5.41	51.59±4.39	−3.482	0.001
	Foveal area	30.51±7.66	33.35±6.42	−2.016	0.046
	Parafoveal area	53.64±4.29	55.27±3.36	−2.126	0.036
	Perifoveal area	49.70[46.00;53.80]	53.50[49.10;56.45]	−3.045	0.002

Notes: Whole: the overall vascular density within 6mm of the macular fovea; Foveal area refers to the density of a circular area with a diameter of 1mm; parafoveal area refers to the density of a ring-shaped area with a diameter of 1–3mm; perifoveal area refers to the density of a ring-shaped area with a diameter of 3–6mm.For data conforming to the normal distribution, expressed as x±s, the independent sample *t*-test was used; for non-normal distribution, expressed as median [upper fourth-lower fourth], the Mann–Whitney *U*-test was used.
Abbreviations: VD, vascular density; SCP, superficial capillary plexus; DCP, deep capillary plexus.

https://doi.org/10.2147/IJGM.S534255

Table 3 Comparison Vascular Density of SCP in the Macular Area Between the Two Subject Groups

SCP	Vascular Density (%)	LI Group (N=49)	Control Group (N=51)	t/z	P Value
Parafoveal area	Temporal	50.40 [46.50;52.10]	53.00 [50.65;54.55]	−3.969	<0.001
	Superior	51.20 [47.20;53.30]	54.70 [52.90;56.75]	−5.189	<0.001
	Nasal	49.30 [45.30;51.30]	51.60 [50.45;53.30]	−4.117	<0.001
	Inferior	51.40 [44.10;53.50]	54.30 [52.70;56.30]	−4.472	<0.001
Perifoveal area	Temporal	44.40 [42.30;47.30]	48.20 [46.85;49.75]	−5	<0.001
	Superior	48.50 [46.00;50.90]	52.40 [50.85;53.70]	−5.766	<0.001
	Nasal	51.50 [48.80;53.70]	54.80 [53.55;56.60]	−5.424	<0.001
	Inferior	48.70 [44.80;50.10]	52.30 [49.80;53.50]	−5.22	<0.001

Notes: The parafoveal and perifoveal areas were divided into four regions using four radial divisions: the temporal, superior, nasal, and inferior regions.
Abbreviations: VD, vascular density; DCP, deep capillary plexus; VD, vascular density; DCP, deep capillary plexus.

Table 4 Comparison Vascular Density of DCP in the Macular Area Between the Two Subject Groups

DCP	Vascular Density (%)	LI Group (N=49)	Control Group (N=51)	t/z	P Value
Parafoveal area	Temporal	54.52±3.67	55.82±3.38	−1.846	0.068
	Superior	54.30 [49.70;57.70]	55.40 [52.10;57.65]	−1.4	0.162
	Nasal	54.40 [51.90;57.30]	56.40 [53.75;58.65]	−2.207	0.027
	Inferior	52.63±5.23	54.02±4.05	−1.491	0.139
Perifoveal area	Temporal	52.60 [49.70;56.30]	55.00 [52.65;58.60]	−3.134	0.002
	Superior	49.60 [45.30;54.30]	54.40 [49.45;57.35]	−3.503	<0.001
	Nasal	48.57±6.57	50.99±5.58	−1.988	0.05
	Inferior	47.10 [42.70;53.10]	53.60 [48.15;56.90]	−3.207	0.001

Abbreviations: DCP, deep capillary plexus; VD, vascular density; DCP, deep capillary plexus.

Table 5 Comparison FAZ and GCC Thickness in the Macular Area Between the Two Subject Groups

	LI Group (N=49)	Control Group (N=51)	t/z	P Value
FAZ area (mm2)	0.34±0.11	0.33±0.09	0.382	0.704
PERIM (mm)	2.25±0.39	2.22±0.32	0.387	0.7
AI	1.10 [1.08;1.13]	1.10 [1.09;1.11]	−0.344	0.731
GCC thickness (μm)	94.88±7.37	100.53±4.61	−4.617	<0.001
CVI (%)	65.78 [64.30;67.42]	67.12 [65.60;67.79]	−2.007	0.045

Abbreviations: GCC, ganglion cell complex; FAZ, foveal avascular zone; PERIM, FAZ perimeter; AI, A-circularity index; LI, lacunar cerebral infarction; CVI, calculate choroidal vascular index.

likelihood of lacunar cerebral infarction (OR < 1, p < 0.05), An increase in diastolic pressure is significantly associated with an increased probability of lacunar cerebral infarction (OR > 1, p < 0.05), as shown in Table 6.

ROC Curve Analysis Was Used to Evaluate the Predictive Efficacy of Macular Microvascular Changes and GCC Thickness in Symptomatic Lacunar Cerebral Infarction

Analysis showed that the diastolic pressure AUC = 0.624, cut-off value = 72.5, sensitivity = 21.6%, specificity = 98%, the whole VD of SCP AUC = 0.856, cut-off value = 49.85, sensitivity = 78.40%, specificity = 79.60%, GCC thickness AUC = 0.754, cut-off value =95.5, sensitivity = 90.2%, specificity = 55.1%, We combined the indicators of the whole VD

Table 6 Correlation Between Macular Microvascular Parameters and the Occurrence of Symptomatic Lacunar Cerebral Infarction

	B-Value	P- Value	OR-Value	95% CI Lower Limit	95% CI Upper Limit
Diastolic pressure (mmHg)	0.074	0.024	1.077	1.01	1.148
The whole VD of SCP	−0.623	<0.001	0.536	0.401	0.718
GCC thickness (um)	−0.126	0.019	0.882	0.794	0.98
Constant	37.03	<0.001	1.20741E+16		

Abbreviations: SCP, superficial capillary plexus; GCC, ganglion cell complex; VD, vascular density; the whole VD, VD of Foveal area +Parafoveal area+Perifoveal area.

Table 7 Predictive Ability of Macular Microvascular Changes and GCC Thickness, Diastolic Pressurefor the Occurrence of Symptomatic Lacunar Cerebral Infarction

	AUC	p Value	95% CI Lower Limit	95% CI Upper Limit
Diastolic pressure (mmHg)	0.624	0.033	0.515	0.733
GCC thickness (um)	0.754	<0.001	0.654	0.855
The whole VD of SCP	0.856	<0.001	0.782	0.929
GCC thickness +Whole VD of SCP	0.88	<0.001	0.813	0.947

Abbreviations: SCP, superficial capillary plexus; GCC, ganglion cell complex; VD, vascular density; the whole VD, VD of Foveal area+Parafoveal area+Perifoveal area.

of SCP and GCC thickness, and the area under the curve of GCC thickness + the whole VD of SCP was further increased (AUC = 0.880, sensitivity = 87.80%, specificity =74.50%). Table 7 presents the ROC curves for the whole VD of SCP and the GCC thickness and GCC thickness +the Whole VD of SCP are illustrated in Figure 4.

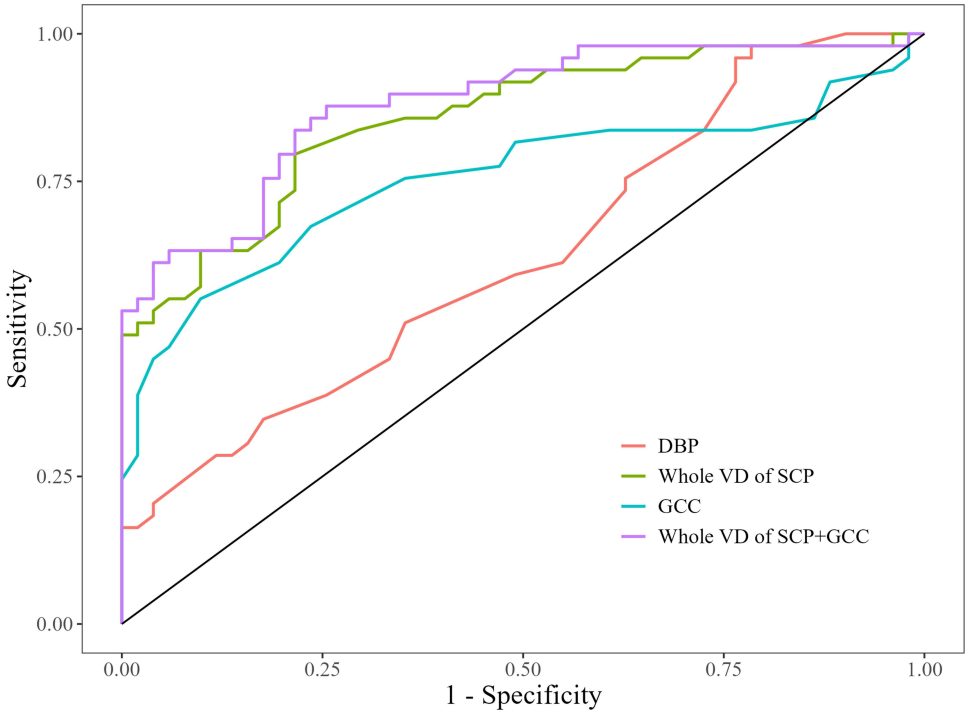

Figure 4 ROC curves of macular microvascular parameters and GCC thickness for predicting the occurrence of symptomatic lacunar cerebral infarction.ROC curves of the whole VD of SCP, GCC thickness and combination of the GCC thickness and the whole VD of the SCP in predicting the occurrence of symptomatic lacunar cerebral infarction.

Abbreviations: ROC, receive operating characteristic; SCP, superficial capillary plexus; VD, vascular density; GCC, ganglion cell complex; the whole VD, VD of Foveal area +Parafoveal area+Perifoveal area.

https://doi.org/10.2147/IJGM.S534255

Discussion

In the current study, we investigated changes in fundus microvascular density and GCC thickness in patients with symptomatic LI and assessed whether these measurements could be used as ocular biomarkers to predict symptomatic LI. This study indicate that reduced retinal VD and GCC thickness, increased diastolic and systolic pressure, the whole VD of SCP and GCC thickness were a strong predictor of symptomatic LI, and that the combination GCC thickness and the whole VD of SCP could further improve discrimination. In conclusion, we believe that OCTA may be a potentially useful tool for predicting LI and allowing timely intervention and treatment of cerebrovascular events using non-invasive imaging techniques.

The results of the study showed that the differences in both systolic and diastolic blood pressure between symptomatic LI patients and normal controls were statistically significant (see Table 1). Our results are consistent with previous studies.[28] These findings highlight the importance of optimising blood pressure management in patients with LI.

Our first major finding was that the whole VD of SCP and DCP was significantly lower than control ($p < 0.05$), which aligns with the findings of Kwapong et al[23] and Zhang et al.[29] Prior studies have demonstrated that the narrowing of small arteries or focal arterioles serves as a sensitive biomarker linked to the development of cerebral small vessel disease(CSVD)[30] and acts as a predictive indicator for lacunar stroke.[31,32] Pachade et al analysed macular microvascular density features using OCTA and fundus images, reporting a decrease in retinal microvascular density among patients with acute stroke.[33] LI is associated with small artery stenosis, and patients with retinal small artery stenosis are expected to exhibit reduced microvascular blood flow in the macular region, potentially reflected in OCTA as a decrease in VD. In consistent with that, This research indicates that the vascular density in the macular area of LI patients is lower. Additionally, we further partitioned the macula and discovered that the area of decreased VD in the SCP layer was more extensive (Figure 2B). Binary logistic regression analysis indicated that lower VD in the SCP and along with reduced GCC thickness, elevated diastolic blood pressure, were significantly associated with symptomatic LI ($OR < 1$, $p < 0.05$)(Table 6). The ROC curve analysis showed that the area under the curve (AUC) was higher for SCP vascular density and GCC thickness, so the two metrics were combined and the area under the curve was highest for SCP+GCC, with an AUC of 0.880. The whole VD of SCP and GCC thickness may serve as a sensitive ocular biomarker for symptomatic LI.

The DCP comprises retinal capillaries of uniform size, with each capillary unit surrounded by endothelial cells and pericytes.[34–36] These two cell types possess self-regulatory features that help maintain stable blood flow during retinal hypoperfusion.[37] We speculate that this is also the reason why deep blood flow density is less susceptible to external factors. As this study is observational, we have not explored the contributing mechanism.

The thickness of the GCC functions not just as a marker for glaucoma, but additionally plays a role in monitoring diseases related to retinal microcirculation.[38,39] Retinal ganglion cells (RGCs), which are the main neurons that output signals from the retina, convey neurotransmitter messages to the brain through the optic nerve.[40] Due to the shared origins and close anatomical relationships between the retina and the brain, patients with various neurodegenerative and systemic diseases often exhibit thinning of RGCs. Consequently, it is hypothesized that the thinning of RGCs may reflect alterations in the central nervous system of these patients.[40,41] The present study showed that GCC thickness was reduced in symptomatic LI patients compared to healthy subjects, which is consistent with the findings of Kwapong WR.[33] and Zhang et al.[34] The possible factors as outlined below: the retinal ganglion cell layer shows increased sensitivity to acute, transient, and mild hypoxic stress occurring systemically.[42] And the SCP provides both nutrients and oxygen to the nerve fiber layer and ganglion cells within the retina.[43] In patients with low perfusion LI, the VD of the SCP decreased, resulting in altered blood supply and oxygenation in the corresponding retinal area. This low perfusion and hypoxia are believed to contribute to a reduction in GCC thickness.

The accessibility of FAZ indicators in clinical practice has led to their frequent utilisation for the observation of alterations in the FAZ region associated with neurodegenerative diseases, hypertension, and cerebrovascular diseases.[15,23,44] In this study, no significant difference was observed in the FAZ area between the symptomatic LI group and the healthy control group, which contradicts previous research findings. In the 2021 Kwapong study, researchers examined 22 patients with cerebral infarction. The OCTA (Avanti RTVue-XR) retinal scan area was defined as a 3×3 mm² region centered on the macula.[23] In the 2022 DUAN study involving 14 patients with non-lacunar infarction and 19 with lacunar infarction, the OCT system used a 3×3 mm² macular-centered scanning area.[45] This study exclusively focused on lacunar infarction cases, and the severity of cerebrovascular disease was lower than that of the above two studies. Notably, our OCTA scan area was expanded to 6×6 mm²,

differing from the previous research protocols. Additionally, our sample size significantly exceeded those of the prior studies. These differences may explain the discrepancies in research outcomes.

This study revealed that, compared with healthy controls, symptomatic LI patients exhibited a decreased CVI. Recent studies have indicated that internal carotid artery stenosis leads to hypoperfusion of the choroidal vessels, and that changes in the choroid correlate with alterations in cerebral hemodynamics, and vice versa.[46] During the progression of ischemic cerebrovascular disease, vascular dysfunction in insufficient cerebral perfusion[47] establishing a cascading relationship between cerebral and retinal perfusion. We speculate that long-term inadequate perfusion leads to a decrease in the choroidal vascular index. However, the mechanisms underlying these choroidal changes remain unclear, as the choroid consists of a highly coordinated network of capillaries[48] and its circulation is regulated by neurogenic factors, innervated by both the sympathetic and parasympathetic nervous systems.[49] The parasympathetic control of vascular dilation facilitates an increase in blood flow. Furthermore, studies involving patients with Parkinson's disease (PD) suggest that variations in the CVI may also be linked to the dysregulation of neurotransmitters[50] that govern normal choroidal perfusion, including dopamine[51] and acetylcholine.[52] We propose that the reduction in choroidal blood flow observed in symptomatic LI patients may be attributable to neurological damage and vascular lesions resulting from cerebral infarction, warranting further research to substantiate this hypothesis.

In this study, we utilized Optical Coherence Tomography with Angiography (RTVue-XR Avanti) to examine retinal microvascular structures in the macula of LI patients. OCTA employs the Split Spectral Amplitude Correlation (SSADA) algorithm to evaluate retinal microvessels, converting complex vascular patterns into precise data metrics.[20,53] This approach not only facilitates comparative analysis between different samples but also ensures the rationality and reliability of results. Consequently, our research demonstrates high reliability and validity by quantifying retinal microvascular structures in LI patients through OCTA and correlating them with brain structural features. This innovative method provides a non-invasive, convenient evaluation approach for early diagnosis of LI, contributing to its prevention and treatment. It aids in understanding the correlation between retinal biomarkers and systemic diseases while offering additional early biomarkers.

Conclusion

This study indicates that the decrease in the whole VD of the SCP and GCC thickness, along with the increase in diastolic blood pressure, possesses predictive value for symptomatic lacunar cerebral infarction (LI).

Retinal microvascular abnormalities may serve as ocular biomarkers for symptomatic LI, facilitating the screening of high-risk populations, enhancing risk awareness education, guiding treatment interventions, and potentially preventing further progression to stroke.

Abbreviations

OCTA, optical coherence tomography angiography; LI, lacunar cerebral infarction; EDI-OCT, Enhanced depth imaging optical coherence tomography; SCP, superficial capillary plexus; DCP, deep capillary plexus; GCC, ganglion cell complex; CVI, choroidal vascular index; FAZ, the foveal avascular zone; PERIM, the perimeter of the FAZ; AI, A-circularity index.

Data Sharing Statement

The data that support the findings of this study are available from the corresponding author Haiyang Liu upon reasonable request.

Ethics Declarations

This study was approved by the Institutional Review Board of Xuzhou First People's Hospital (Ethical approval number: xyyll【2023】057). Informed consent was obtained from all subjects. All methods were conducted in accordance with the tenets of the Declaration of Helsinki.

Author Contributions

H.L generalized the idea of the new research, and revised the manuscript. N.W recommend patients for enrollment. H.X, M.L and G.R analyzed and interpreted the patient data, and drafted the manuscript. R.G and M.L contributed to the acquisition and analysis of data. L.G, D.Z and R.G interpreted the results and edited the photos. Y.H reviewed and revised the manuscript. All authors made a significant contribution to the work reported, whether that is in the conception, study design, execution, acquisition of data, analysis and interpretation, or in all these areas; took part in drafting, revising or critically reviewing the article; gave final approval of the version to be published; have agreed on the journal to which the article has been submitted; and agree to be accountable for all aspects of the work.

Funding

This study was supported by Xuzhou Medical Key Talents Project (No. XWRCHT20220048), Xuzhou Key R & D Program (No. KC22099) and Basic Research Program of Jiangsu (BK20241765).

Disclosure

The authors declare no competing interests in this work.

References

1. Ohlmeier L, Nannoni S, Pallucca C, et al. Prevalence of, and risk factors for, cognitive impairment in lacunar stroke. *Int J Stroke*. 2023;18(1):62–69. doi:10.1177/17474930211064965
2. Zhou Y, Gao H, Zhao F, et al. The study on analysis of risk factors for severity of white matter lesions and its correlation with cerebral microbleeds in the elderly with lacunar infarction. *Medicine*. 2020;99(4):e18865. doi:10.1097/MD.0000000000018865
3. Paradise MB, Shepherd CE, Wen W, Sachdev PS. Neuroimaging and neuropathology indices of cerebrovascular disease burden: a systematic review. *Neurology*. 2018;91(7):310–320. doi:10.1212/WNL.0000000000005997
4. Ji Y, Ji Y, Liu Y, Zhao Y, Zhang L. Research progress on diagnosing retinal vascular diseases based on artificial intelligence and fundus images. *Front Cell Develop Biol*. 2023;11:1168327. doi:10.3389/fcell.2023.1168327
5. Gao Y, Xu L, He N, et al. A narrative review of retinal vascular parameters and the applications (Part I): measuring methods. *Brain Circ*. 2023;9(3):121–128. doi:10.4103/bc.bc_8_23
6. Patton N, Aslam T, Macgillivray T, et al. Retinal vascular image analysis as a potential screening tool for cerebrovascular disease: a rationale based on homology between cerebral and retinal microvasculatures. *J Anatomy*. 2005;206(4):319–348. doi:10.1111/j.1469-7580.2005.00395.x
7. Rim TH, Teo AWJ, Yang HHS, Cheung CY, Wong TY. Retinal vascular signs and cerebrovascular diseases. *J Neuroophthalmol*. 2020;40(1):44–59. doi:10.1097/WNO.0000000000000888
8. Zhao L, Yanan C, Bin J, Saiguang L, Yanling W. Correlation analysis between retinal vascular morphology parameters and ischemic stroke Chinese. *J Ocular Dis*. 2022. doi:10.3760/cma.j.cn511434-20220919-00502
9. Huang KK, Huang S, Yun WW, et al. Correlation between total cerebral small vessel disease score and retinal vessel diameters in patients with mild stroke. *Zhonghua yi xue za zhi*. 2021;101(1):62–67. doi:10.3760/cma.j.cn112137-20200405-01088
10. Wardlaw JM, Smith C, Dichgans M. Small vessel disease: mechanisms and clinical implications. *Lancet Neurol*. 2019;18(7):684–696. doi:10.1016/S1474-4422(19)30079-1
11. Spaide RF, Fujimoto JG, Waheed NK, Sadda SR, Staurenghi G. Optical coherence tomography angiography. *Prog Retinal Eye Res*. 2018;64:1–55. doi:10.1016/j.preteyeres.2017.11.003
12. Um T, Seo EJ, Kim YJ, Yoon YH. Optical coherence tomography angiography findings of type 1 diabetic patients with diabetic retinopathy, in comparison with type 2 patients. *Graefe's Arch Clin Exp Ophthalmol*. 2020;258(2):281–288. doi:10.1007/s00417-019-04517-6
13. Aschauer J, Aschauer S, Pollreisz A, et al. Identification of subclinical microvascular biomarkers in coronary heart disease in retinal imaging. *Trans Vision Sci Technol*. 2021;10(13):24. doi:10.1167/tvst.10.13.24
14. Di Pippo M, d'Agostino S, Ruggeri F, et al. Parkinson's disease: what can retinal imaging tell us? *J Integrative Neurosci*. 2024;23(1):23. doi:10.31083/j.jin2301023
15. Lee J, Kim JP, Jang H, et al. Optical coherence tomography angiography as a potential screening tool for cerebral small vessel diseases. *Alzheimer's Res Ther*. 2020;12(1):73. doi:10.1186/s13195-020-00638-x
16. Kawasaki R, Che Azemin MZ, Kumar DK, et al. Fractal dimension of the retinal vasculature and risk of stroke: a nested case-control study. *Neurology*. 2011;76(20):1766–1767. doi:10.1212/WNL.0b013e31821a7d7d
17. Liew G, Gopinath B, AJ White, et al. Retinal Vasculature Fractal and Stroke Mortality. *Stroke*. 2021;52(4):1276–1282. doi:10.1161/STROKEAHA.120.031886
18. Li X, Zhu S, Zhou S, et al. Optical coherence tomography angiography as a noninvasive assessment of cerebral microcirculatory disorders caused by carotid artery stenosis. *Dis Markers*. 2021;2021:2662031. doi:10.1155/2021/2662031
19. Zhao Y, Dong D, Yan D, et al. Increased retinal venule diameter as a prognostic indicator for recurrent cerebrovascular events: a prospective observational study. *Neural Regeneration Res*. 2024;19(5):1156–1160. doi:10.4103/1673-5374.382863
20. Huang D, Jia Y, Gao SS, Lumbroso B, Rispoli M. Optical coherence tomography angiography using the optovue device. *Develop Ophthalmol*. 2016;56:6–12. doi:10.1159/000442770
21. Yao H, Li Z. Is preclinical diabetic retinopathy in diabetic nephropathy individuals more severe? *Front Endocrinol*. 2023;14:1144257. doi:10.3389/fendo.2023.1144257

22. Abdelhalim AS, Abdelkader MFSO, Mahmoud MSE, Mohamed Mohamed AA. Macular vessel density before and after panretinal photocoagulation in patients with proliferative diabetic retinopathy. *Int J Retina Vitreous*. 2022;8(1):21. doi:10.1186/s40942-022-00369-1
23. Kwapong WR, Yan Y, Hao Z, Wu B. Reduced superficial capillary density in cerebral infarction is inversely correlated with the NIHSS score. *Front Aging Neurosci*. 2021;13:626334. doi:10.3389/fnagi.2021.626334
24. Guan R, Qin S, Chi Y, Tang Z, Liu H. Application of optical coherence tomography angiography to study retinal and choroidal vascular changes in patients with first-time coronary artery stenosis. *Photodiagn Photodyn Ther*. 2025;51:104435. doi:10.1016/j.pdpdt.2024.104435
25. Liu L, Gao J, Bao W, et al. Analysis of foveal microvascular abnormalities in diabetic retinopathy using optical coherence tomography angiography with projection artifact removal. *J Ophthalmol*. 2018;2018:3926745. doi:10.1155/2018/3926745
26. Lin C, Yang Z, Chen C, et al. Reduced macular vessel density and inner retinal thickness correlate with the severity of cerebral autosomal dominant arteriopathy with subcortical infarcts and leukoencephalopathy (CADASIL). *PLoS One*. 2022;17(5):e0268572. doi:10.1371/journal.pone.0268572
27. Chen J, Guan L, Liu Y, et al. Choroidal vascular changes in silicone oil-filled eyes after vitrectomy for rhegmatogenous retinal detachments. *BMC Ophthalmol*. 2023;23(1):442. doi:10.1186/s12886-023-03167-x
28. Rakotomanana JL, Randrianantoandro NR, Rasaholiarison NF, et al. Correlation between silent lacunar strokes and retinopathies seen on fundus among patients hospitalized for lacunar strokes: an observational study at the neurology department of Befelatanana university hospital. *J de Med Vasculaire*. 2022;47(5–6):250–255. doi:10.1016/j.jdmv.2022.10.011
29. Zhang X, Xiao H, Liu C, et al. Optical coherence tomography angiography reveals distinct retinal structural and microvascular abnormalities in cerebrovascular disease. *Front Neurosci*. 2020;14:588515. doi:10.3389/fnins.2020.588515
30. Rodríguez I, Lema I, Blanco M, et al. Vascular retinal, neuroimaging and ultrasonographic markers of lacunar infarcts. *Int J Stroke*. 2010;5 (5):360–366. doi:10.1111/j.1747-4949.2010.00462.x
31. Lindley RI, Wang JJ, Wong M, et al. Retinal microvasculature in acute lacunar stroke: a cross-sectional study. *Lancet Neurol*. 2009;8(7):628–634. doi:10.1016/S1474-4422(09)70131-0
32. Yatsuya H, Folsom AR, Wong TY, et al. Retinal microvascular abnormalities and risk of lacunar stroke: atherosclerosis risk in communities study. *Stroke*. 2010;41(7):1349–1355. doi:10.1161/STROKEAHA.110.580837
33. Pachade S, Coronado I, Abdelkhaleq R, et al. Detection of stroke with retinal microvascular density and self-supervised learning using OCT-A and fundus imaging. *J Clin Med*. 2022;11(24):7408. doi:10.3390/jcm11247408
34. Campbell JP, Zhang M, Hwang TS, et al. Detailed vascular anatomy of the human retina by projection-resolved optical coherence tomography angiography. *Sci Rep*. 2017;7(1):42201. doi:10.1038/srep42201
35. Gardiner TA, Archer DB, Curtis TM, Stitt AW. Arteriolar involvement in the microvascular lesions of diabetic retinopathy: implications for pathogenesis. *Microcirculation*. 2007;14(1):25–38. doi:10.1080/10739680601072123
36. Edwards NFA, Scalia GM, Shiino K, et al. Global myocardial work is superior to global longitudinal strain to predict significant coronary artery disease in patients with normal left ventricular function and wall motion. *J American Soc Echocardiography*. 2019;32(8):947–957. doi:10.1016/j.echo.2019.02.014
37. Chakravarthy U, Gardiner TA. Endothelium-derived agents in pericyte function/dysfunction. *Prog Retinal Eye Res*. 1999;18(4):511–527. doi:10.1016/s1350-9462(98)00034-2
38. Lo J, Mehta K, Dhillon A, et al. Therapeutic strategies for glaucoma and optic neuropathies. *Mol Aspect Med*. 2023;94:101219. doi:10.1016/j.mam.2023.101219
39. Lim HB, Lee MW, Park JH, et al. Changes in ganglion cell–inner plexiform layer thickness and retinal microvasculature in hypertension: an optical coherence tomography angiography study. *Am J Ophthalmol*. 2019;199:167–176. doi:10.1016/j.ajo.2018.11.016
40. Gu YX, Chen M, Wang KJ. Research advances in classifications and functions of retinal ganglion cells. *[Zhonghua yan ke za zhi] Chinese J Ophthalmol*. 2022;58(5):390–395. doi:10.3760/cma.j.cn112142-20211103-00516
41. London A, Benhar I, Schwartz M. The retina as a window to the brain-from eye research to CNS disorders. *Nat Rev Neurol*. 2013;9(1):44–53. doi:10.1038/nrneurol.2012.227
42. Kergoat H, Hérard M, Lemay M. RGC sensitivity to mild systemic hypoxia. *Invest Ophthalmol Visual Sci*. 2006;47(12):5423–5427. doi:10.1167/iovs.06-0602
43. Cabrera DeBuc D, Somfai GM, Koller A. Retinal microvascular network alterations: potential biomarkers of cerebrovascular and neural diseases. *Am J Physiol Heart Circulatory Physiol*. 2017;312(2):H201–H212. doi:10.1152/ajpheart.00201.2016
44. Huang S, Zhang S, Wang J, Hou G, Xu S. Correlation between serum cystatin c level and retinal blood flow in patients with essential hypertension. *Ophthalmic Res*. 2022;65(3):335–341. doi:10.1159/000522219
45. Duan H, Xie J, Zhou Y, et al. Characterization of the retinal microvasculature and FAZ changes in ischemic stroke and its different types. *Trans Vision Sci Technol*. 2022;11(10):21. doi:10.1167/tvst.11.10.21
46. Sampson DM, Gong P, An D, et al. Axial length variation impacts on superficial retinal vessel density and foveal avascular zone area measurements using optical coherence tomography angiography. *Invest Ophthalmol Visual Sci*. 2017;58(7):3065–3072. doi:10.1167/iovs.17-21551
47. Liu J, Zhu Y, Wu Y, et al. Association of carotid atherosclerosis and recurrent cerebral infarction in the Chinese population: a meta-analysis. *Neuropsychiatr Dis Treat*. 2017;13:527–533. doi:10.2147/NDT.S124386
48. Nickla DL, Wallman J. The multifunctional choroid. *Prog Retinal Eye Res*. 2010;29(2):144–168. doi:10.1016/j.preteyeres.2009.12.002
49. Kaštelan S, Orešković I, Bišćan F, Kaštelan H, Gverović Antunica A. Inflammatory and angiogenic biomarkers in diabetic retinopathy. *Biochemia medica*. 2020;30(3):030502. doi:10.11613/BM.2020.030502
50. Kwapong WR, Ye H, Peng C, et al. Retinal microvascular impairment in the early stages of Parkinson's disease. *Invest Ophthalmol Visual Sci*. 2018;59(10):4115–4122. doi:10.1167/iovs.17-23230
51. Huemer K, Zawinka C, Garhöfer G, et al. Effects of dopamine on retinal and choroidal blood flow parameters in humans. *Br J Ophthalmol*. 2007;91 (9):1194–1198. doi:10.1136/bjo.2006.113399
52. Zhang Z, Zhou Y, Xie Z, et al. The effect of topical atropine on the choroidal thickness of healthy children. *Sci Rep*. 2016;6(1):34936. doi:10.1038/srep34936
53. Wang H, Liu X, Hu X, et al. Retinal and choroidal microvascular characterization and density changes in different stages of diabetic retinopathy eyes. *Front Med*. 2023;10:1186098. doi:10.3389/fmed.2023.1186098